

Chapter 7

Quantum Cryptography

This chapter was previously published as
S. Zhao and H. De Raedt, *J. Comp. Theor. Nanosci.* **5**, 490504 (2008).

7.1 Introduction

Cryptography is an artifice of exchanging information between two parties such that an unauthorized person cannot retrieve this information. To this end, the sender usually employs some key to encrypt the information to be transmitted, and the receiver applies a decryption algorithm to recover the original information. If the cryptographic system is secure, an eavesdropper can decipher the encrypted message if and only if the eavesdropper knows the key. Thus, the central problem of cryptography is to establish a powerful key. We may imagine that the more bits the key contains and the more complicated the key is, the more secure the process is. But, in practice, if the key is generated and transmitted in a conventional, electronic way, it may be possible to intercept the key. Then, the eavesdropper can make a copy of the exchanged information without changing it, such that the sender or the receiver did not notice that the information has been intercepted.

Quantum cryptography uses microscopic objects such as individual photons as information carriers [135]. One of the characteristic features of such microscopic systems

is that a measurement may change the information that the microscopic system carries. Therefore, if an eavesdropper attempts to make a measurement to determine a bit of the key, there is no guarantee that the information carried by the microscopic system is left unchanged. If the quantum cryptography protocol is designed properly, the presence of the eavesdropper is revealed by an increase of the error rate in the bits that are being transmitted from sender to receiver.

Although there is no doubt that quantum theory is very successful in describing a vast number of experimental results, it is well-known that quantum theory has nothing to say about individual events that are being recorded in experiments [1, 2]. Yet, quantum cryptography uses individual events to transmit information, its security being guaranteed by axioms. Since the inception of quantum theory, the major fundamental problem of incorporating in quantum theory the fact that we observe events only is often referred to as the quantum measurement paradox and has not yet found a solution within the realm of quantum theory [1]. Therefore, it seems worthwhile the study the fundamental question what it is that makes quantum cryptography work: Logically speaking, it cannot be quantum mechanics because quantum mechanics has nothing to say about individual events [1, 2].

In a number of recent papers [17–20, 63, 69, 70, 136], we have demonstrated that locally-connected networks of processing units can simulate, event-by-event, the single-photon beam splitter, Mach-Zehnder interferometer experiments of Grangier *et al.* [16], and Einstein-Podolsky-Rosen experiments with photons [44, 45]. Furthermore, we have shown that this approach can be generalized to simulate universal quantum computation [95] by an event-by-event process [18, 20]. Therefore, this suggests that at least in principle, it may be possible to simulate all wave interference phenomena and many-body quantum systems using particle-like processes only. In this paper, we extend this approach to quantum cryptography systems.

This chapter is structured as follows. In Sections 7.2 and 7.3, we briefly review the two most popular protocols of quantum cryptography: the BB84 protocol [137–139] and Ekert’s protocol [140]. Although both protocols are closely related [135], from the point of view of simulation algorithm, the latter is considerably more complicated than the former, which is the main reason for discussing both of them. The simulation algorithms for the polarizer are presented in Section 7.4. Simulation results for the BB84 and the Ekert protocol, both with and without eavesdropper, are given in Sections 7.5 and 7.6. Although our simulation method does not rely on any concept of quantum theory, it is nevertheless capable of simulating quantum cryptography protocols on the event-by-event level. Therefore, it may shine light on the question what is essential for quantum cryptography to work. In Section 7.5.4, we discuss this issue. The results of this chapter are summarized in Section 7.7.

Table 7.1: Summary of the BB84 protocol. The first column shows the bit that Alice wants to encode and send to Bob. The second and third columns give the orientations of Alice’s and Bob’s polarizers, respectively. The fourth and fifth columns are the probabilities that Bob detects a photon in the output channel 0 and 1 of his polarizer. The last column gives the bit that Bob obtains from his measurement. The question mark indicates that the probability that Bob makes the wrong guess is 50%.

Alice’s bit	ϕ_A	ϕ_B	P_0	P_1	Bob’s bit
			$\cos^2(\phi_A - \phi_B)$	$\sin^2(\phi_A - \phi_B)$	
0	0^0	0^0	1	0	0
		45^0	1/2	1/2	?
0	45^0	0^0	1/2	1/2	?
		45^0	1	0	0
1	90^0	0^0	0	1	1
		45^0	1/2	1/2	?
1	135^0	0^0	1/2	1/2	?
		45^0	0	1	1

7.2 BB84 protocol

In 1989, an experimental prototype that implemented the quantum cryptography protocol BB84 [137–139], demonstrated that it is possible to transmit an encryption key using the polarization state of single photons. In this section, we briefly review the idea behind this protocol.

The BB84 protocol employs the polarization state of photons as the information carrier. As each detection of a single photon yields one out of two definite answers for the polarization of the photon, these observations can be described by the quantum theory of a two-state system. The BB84 protocol uses two sets of non-orthogonal coordinate systems, which are the usual x - y (rectilinear) basis and the diagonal basis which is the rectilinear basis rotated by 45° . In the rectilinear basis, the photon can be either in the horizontal (\longrightarrow) or in the vertical (\uparrow) polarization state. In the diagonal linear basis, the photon can be either in the diagonal (\nearrow) or in the anti-diagonal (\nwarrow) polarization state.

Let Alice and Bob be the two parties who want to exchange a secret key. Alice generates and sends Bob a sequence of photons with polarization states that are selected randomly from the four possible directions: $0^0(\longrightarrow)$, $45^0(\nearrow)$, $90^0(\uparrow)$ and $135^0(\nwarrow)$. The bits of Alice are encoded from these directions in the following way: 0^0 and 45^0 represent bit 0, 90^0 and 135^0 represent bit 1. When a photon arrives at Bob’s observation station, Bob performs a measurement on this photon based on a

randomly selected basis, either the rectilinear or the diagonal basis. Bob encodes the outcome of his measurements in the same way as Alice does. If Bob chooses a basis which is consistent with Alice selection (for instance, Alice's sends a photon polarized in 0^0 or 90^0 , and Bob performs the measurement on the rectilinear basis), then it is assumed that Bob's bit is identical to that of Alice. Otherwise Bob will guess the wrong bit for about 50% of the detected photons. Table. 7.1 lists the various possibilities that Alice and Bob may encounter during the exchange of data. It should be clear from this discussion that up to this point, it has been assumed that the detectors operate with 100% detection efficiency, that the coordinate systems of Alice and Bob are perfectly aligned and so on, that is we assume that the experiment is perfect.

After recording a collection of events, in the next step, Alice and Bob will sift the key from the original raw bits by communicating through a conventional classical channel. For each photon that Bob has received, he tells Alice which basis he has selected but he does not tell her the result of the measurement. Then, for each photon, Alice announces to Bob whether he made a correct choice. Finally they discard all the bits for which Bob has made the wrong choice of basis. The bits that survive the sifting procedure constitute the key and be used to encrypt the data that they want to send to each other.

An eavesdropper, conventionally called Eve, who attempts to intercept some photons during the key transmission process will cause some errors in the sifted key, and these errors can be detected by Alice and Bob through publicly comparing randomly selected subsets of their sifted key. If Eve performs the similar measurements as Bob on all photons sent by Alice, and then prepares and resents new photons according to her measurements, Alice and Bob will observe an error rate of about 25% and conclude that their communication channel is not secure.

7.3 Ekert's protocol

In 1991, Artur Ekert proposed another protocol based on entanglement states with security guaranteed by Bell inequalities [140]. The source can be any two-particle system with some property entangled. In the original proposal of the protocol, pairs of spin- $\frac{1}{2}$ particles in a singlet state are used as the information carrier, but in the real experiments [141, 142], polarization entangled photon pairs are most commonly used to implement this protocol. In Ref. [142], the CHSH inequality (one of the many forms of a Bell inequality) is used to test of the security. In Ref. [141] another form of Bell inequality, the Wigner inequality [143], provides a relative simple test of the security. In this section, we briefly review the main idea of this protocol.

First, it is assumed that there is a source that emits pairs of photons, one photon traveling to Alice and the other photon traveling to Bob. It is assumed that the state

Table 7.2: The quantum theoretical predictions for the single- and two particle probabilities of a system in the singlet state and in the product state. The upper part shows the probability of observing + on one side and the joined probability of observing + on both sides. The lower part gives the expressions for the Wigner parameter S and the modified Wigner parameter S' .

	Singlet state	Product state
$P_+(\phi_A)$	$\frac{1}{2}$	$\cos^2(\psi_A - \phi_A)$
$P_+(\phi_B)$	$\frac{1}{2}$	$\cos^2(\psi_B - \phi_B)$
$P_{++}(\phi_A, \phi_B)$	$\frac{1}{2} \sin^2(\phi_A - \phi_B)$	$\cos^2(\psi_A - \phi_A) \cos^2(\psi_B - \phi_B)$
S	$\sin^2 \theta - \frac{1}{2} \sin^2 2\theta$	$\cos^2 \psi_A \cos^2(\psi_B - \theta) + \cos^2(\psi_A + \theta) \cos^2 \psi_B - \cos^2(\psi_A + \theta) \cos^2(\psi_B - \theta)$
S'	$\sin^2 \theta - \frac{1}{2} \sin^2 2\theta$	$\cos^2 \psi_A \cos^2(\psi_B - \theta) + \cos^2(\psi_A + \theta) \cos^2 \psi_B + \sin^2 \psi_A \sin^2 \psi_B - \cos^2(\psi_A + \theta) \cos^2(\psi_B - \theta)$

of the whole system, that is the description of the observation of the polarization of many pairs, can be described by the singlet state

$$|\Psi\rangle = \frac{1}{\sqrt{2}}(|H\rangle_A |V\rangle_B - |V\rangle_A |H\rangle_B), \quad (7.1)$$

where H and V denote the horizontal and vertical (linear) polarization states. When a pair of photons A and B has been generated at the source, they are spatially separated and sent to Alice and Bob through free air or through some special optical fiber. Then Alice and Bob perform measurements on the polarization state of the received photon using a polarizing beamsplitter. Both Alice and Bob independently and randomly select between two polarization orientations. Let us denote the two orientations of Alice by ϕ_{A_1} and ϕ_{A_2} , and those of Bob by ϕ_{B_1} and ϕ_{B_2} . The outcome for an individual measurement is represented by either +1 or -1. Because of the assumed entanglement between the polarization of the two photons, if Alice and Bob select parallel but otherwise arbitrary orientations of their polarizer, the outcomes of these two measurements are expected to display perfect anticorrelation. Thus, anticorrelation between the two measurements with $\phi_{A_1} = \phi_{B_1}$ can be used to establish the key.

When the two photons of a particular pair are measured in two non-parallel orientations, the correlation between them cannot be recognized as such. Then, we need a test to see if the correlation are those of a system in the singlet state. The Wigner inequality provides a convenient tool to do this. We denote by $P_{++}(\phi_{A_1}, \phi_{B_2})$, $P_{++}(\phi_{A_2}, \phi_{B_1})$, and $P_{++}(\phi_{A_2}, \phi_{B_2})$ the probabilities to obtain +1 on both sides for these three pairs of different orientations of the polarizers. Under the assumptions

discussed in Appendix A these three probabilities must obey Wigner inequality

$$P_{++}(\phi_{A,1}, \phi_{B,2}) + P_{++}(\phi_{A,2}, \phi_{B,1}) - P_{++}(\phi_{A,2}, \phi_{B,2}) \geq 0. \quad (7.2)$$

In Appendix A, we give a simple proof of the Wigner inequality. For later use, it is expedient to define the Wigner parameter by

$$S = P_{++}(\phi_{A,1}, \phi_{B,2}) + P_{++}(\phi_{A,2}, \phi_{B,1}) - P_{++}(\phi_{A,2}, \phi_{B,2}) \quad (7.3)$$

For the singlet state Eq. (7.1), quantum theory predicts that

$$P_{++}(\phi_{A,1}, \phi_{B,1}) = \frac{1}{2} \sin^2(\phi_{A,1} - \phi_{B,1}). \quad (7.4)$$

Inserting Eq. (7.4) into Eq. (7.2), it is easy to check (see later for examples) that for some a range of $\phi_{A,1}$, $\phi_{B,2}$, $\phi_{A,2}$, and $\phi_{B,1}$, we have $S < 0$. Hence the Wigner inequality Eq. (7.2) is violated by a quantum system in the singlet state. For a particular choice of orientations that is used to implement Ekert's protocol namely $\phi_{A,1} = \phi_{B,1} = 0$, $\phi_{A,2} = 30^\circ$, and $\phi_{B,2} = -30^\circ$, we find that $S = -1/8$. Any attempt to tamper with the singlet state will change S from its minimum value $-1/8$ to a larger one.

What happens to the observed data when photons are intercepted and resend? Is the Wigner inequality still powerful enough to reveal the insecurity of the whole system? It turns out that the assumption of perfect anticorrelation, essential for the derivation of Wigner inequality, may cause a security problem. To alleviate this problem, a modified Wigner inequality that does not rely on the assumption of perfect anticorrelation was introduced in Ref. [144]. An experimental test of the power of the modified Wigner inequality in the presence of eavesdropping is given in Ref. [145]. A simple proof of this Modified Wigner inequality is given in Appendix B. Introducing the modified Wigner parameter S' by

$$\begin{aligned} S' &= P_{++}(\phi_{A,1}, \phi_{B,2}) + P_{++}(\phi_{A,2}, \phi_{B,1}) \\ &+ P_{--}(\phi_{A,1}, \phi_{B,1}) - P_{++}(\phi_{A,2}, \phi_{B,2}), \end{aligned} \quad (7.5)$$

the modified Wigner inequality reads

$$S' \geq 0. \quad (7.6)$$

Compared to the original Wigner inequality, an extra term is added which contributes when both Alice and Bob choose the same orientation of their polarizers. This extra term significantly increases the possibility of detecting the presence of an eavesdropper.

For the simulation of this protocol in the presence of eavesdropping, we assume that Eve performs the intercept-resend strategy. This implies that Eve detects the two photons using two polarizers with orientations ψ_A and ψ_B , respectively, and then

uses the result of her measurement of the two photons to prepare a photon that she sends to Alice and another photon that she sends to Bob. According to quantum theory, the photons received by both Alice and Bob are described by the product state

$$|\Psi\rangle = (\cos\psi_A|H\rangle_A + \sin\psi_A|V\rangle_A) \times (\cos\psi_B|H\rangle_B - \sin\psi_B|V\rangle_B). \quad (7.7)$$

The predictions of quantum theory for the product state and the singlet state are summarized in Table 7.2.

In Table 7.2, ϕ_A and ϕ_B denote the orientations of Alice's and Bob's polarizer, respectively, $P_+(\phi_A)$ represents the probability that Alice obtains +1 in her measurement, $P_+(\phi_B)$ denotes the corresponding probability for Bob's measurement, and $P_{++}(\phi_A, \phi_B)$ refers to the probability that both Alice and Bob record a +1 result. In the last two rows of Table 7.2 we list the results of quantum theory for the original and the modified Wigner parameter for the polarizer settings $\phi_{A,1} = \phi_{B,1} = 0$, $\phi_{A,2} = -\theta$, and $\phi_{B,2} = \theta$. For the singlet state, the additional term in the modified Wigner parameter is zero. Hence there is no difference between S and S' and both of them only depend on θ . However in the case of a product state, the additional term $\sin^2\psi_A \sin^2\psi_B$ that depends on the polarization states of the photons and is always non-negative, hence $S' \geq S$. Thus, if Alice and Bob expect to observe the singlet state they should find $S' = S = -1/8$. However, if Eve is intercepting and sending photons in a product state, the modified Wigner inequality provides more power to disclose the existence of an eavesdropper because Eve's actions will cause S' to change from being negative to positive while S may remain negative (see the examples shown later).

7.4 Event-based simulation of a polarizer

Both the practical realization of the BB84 and the Ekert protocol use the detection of the photon polarization. Hence, the polarizer is an indispensable apparatus for both Alice and Bob to perform their measurements. Therefore, to set up an event-by-event computer simulation model for these quantum cryptography protocols, we first need to consider event-based simulation models for a polarizer.

Some optically active materials such as calcite split an incoming beam of light into two spatially separated beams depending on the polarization property of the incident beam [76]. If the incident beam has polarization ψ and the orientation of the polarizer is denoted by ϕ , the intensities of the two output beams 0 and 1 are given by Malus' law

$$\begin{aligned} I_0 &= \cos^2(\psi - \phi), \\ I_1 &= \sin^2(\psi - \phi). \end{aligned} \quad (7.8)$$

Table 7.3: The first 100 bits of the sifted key of the BB84 protocol without eavesdropping. The upper part gives bits 0 – 50, the lower part gives bits 51 – 100. As expected, the sifted key of Alice is identical to the one obtained by Bob.

Alice's bits	1	0	0	0	0	0	0	1	1	1	0	0	1	1	1	0	0	1	1	0
Bob's bits	1	0	0	0	0	0	0	1	1	1	0	0	1	1	1	0	0	1	1	0
Alice's bits	1	1	0	0	0	1	1	0	1	0	0	0	0	1	0	0	1	1	1	0
Bob's bits	1	1	0	0	0	1	1	0	1	0	0	0	0	1	0	0	1	1	1	0
Alice's bits	1	0	1	1	1	0	1	0	1	0	1	0	1	1	1	1	1	1	0	1
Bob's bits	1	0	1	1	1	0	1	0	1	0	1	0	1	1	1	1	1	1	0	1
Alice's bits	0	0	1	0	1	0	1	0	1	1	0	1	0	0	1	0	1	1	1	1
Bob's bits	0	0	1	0	1	0	1	0	1	1	0	1	0	0	1	0	1	1	1	1
Alice's bits	1	0	1	1	1	0	1	1	1	0	0	1	0	1	0	0	0	0	1	0
Bob's bits	1	0	1	1	1	0	1	1	1	0	0	1	0	1	0	0	0	0	1	0

The polarization of output beam 0 is ϕ , and the polarization of output beam 1 is $\phi + \pi/2$. The incident beam is said to be randomly polarized if $I_0 = I_1 = 1/2$.

The simplest simulation model of a polarizer determines the type (0 or 1) of the output by comparing a uniform pseudo-random number r with $\cos^2(\psi - \phi)$. If $r \leq \cos^2(\psi - \phi)$, the output is of type 0, otherwise it is of type 1. For each individual input photon, the outcome is pseudo-random, but if we repeat this process for sufficiently many events (and the pseudo-random number generator is of sufficient quality), the frequencies of observing photons in output 0 and 1 will agree with Malus' law. In the sequel, this model for the polarizer will be called the probabilistic polarizer (PP).

As an alternative for the PP, we will also simulate both protocols using a deterministic model for the polarizer [17–20, 23]. This model will be called the deterministic polarizer (DP). As the details of this model are not of importance for (the analysis of) the results presented in this paper, we refer the reader who is interested in this and other deterministic simulation models for quantum phenomena to Refs. [17–20, 23]. In this paper, we show that both the PP and DP models are capable of reproducing *exactly* all the results of quantum theory for both the BB84 and the Ekert protocol using an event-by-event based simulation algorithm.

7.5 Event-based simulation of the BB84 protocol

In this section, we present the results of an event-by-event simulation of the BB84 protocol using both PPs and DPs. We start with the original BB84 protocol and

Table 7.4: The first 100 bits of the sifted key of the BB84 protocol in the presence of eavesdropping. The upper part gives bits 0 – 50, the lower part gives bits 51 – 100. The differences between Alice’s and Bob’s sifted key are emphasized by underlining the bits. The error rate is about 26%.

Alice’s bits	<u>1</u>	0	1	0	0	0	0	<u>1</u>	0	0	1	<u>1</u>	1	1	0	0	0	0	0	
Bob’s bits	<u>0</u>	0	1	0	0	0	0	<u>0</u>	0	0	1	<u>0</u>	1	1	0	0	0	0	0	
Alice’s bits	<u>1</u>	0	1	0	0	0	0	0	1	<u>1</u>	<u>1</u>	1	0	1	<u>1</u>	1	0	1	1	0
Bob’s bits	<u>0</u>	0	1	0	0	0	0	0	1	<u>0</u>	<u>0</u>	1	0	1	<u>0</u>	1	0	1	1	0
Alice’s bits	<u>1</u>	1	1	0	0	1	1	0	1	1	<u>1</u>	0	1	1	<u>1</u>	1	0	1	<u>0</u>	<u>1</u>
Bob’s bits	<u>0</u>	1	1	0	0	1	1	0	1	1	<u>0</u>	0	1	1	<u>0</u>	1	0	1	<u>1</u>	<u>0</u>
Alice’s bits	0	0	<u>0</u>	<u>0</u>	<u>0</u>	0	1	0	<u>0</u>	1	<u>1</u>	1	0	0	1	0	1	1	0	0
Bob’s bits	0	0	<u>1</u>	<u>1</u>	<u>1</u>	0	1	0	<u>1</u>	1	<u>0</u>	1	0	0	1	0	1	1	0	0
Alice’s bits	1	<u>1</u>	0	<u>0</u>	1	0	1	1	1	0	<u>0</u>	<u>0</u>	<u>1</u>	<u>1</u>	<u>0</u>	<u>1</u>	1	1	<u>0</u>	0
Bob’s bits	1	<u>0</u>	0	<u>1</u>	1	0	1	1	1	0	<u>1</u>	<u>1</u>	<u>0</u>	<u>0</u>	<u>1</u>	<u>0</u>	1	1	<u>1</u>	0

demonstrate that the sifted bits obtained by Alice and Bob are identical, as expected. Then, we simulate the effect of eavesdropping by Eve who uses the intercept-resend strategy and show that this introduces significant errors in the sifted key. Finally, we study the effect of misalignment of the settings of both Alice’s and Bob’s polarizers by computing the fidelity of the sifted key as a function of the misalignment angles.

7.5.1 Simulation of the BB84 protocol in the absence of an eavesdropper

Two polarizers are needed to simulate this protocol, one for Alice, and another one for Bob. Alice uses her polarizer to encode the bits she wants to send by (randomly) selecting the polarization $0^\circ(\rightarrow)$, $45^\circ(\nearrow)$, $90^\circ(\uparrow)$ or $135^\circ(\nwarrow)$. Thus, if Alice wants to encode a random sequence of bits, Alice’s polarizer ϕ_A chooses randomly from these four directions. In the simulation, we use uniform pseudo-random numbers to select the polarizations, implying that half of the photons leave the polarizer through output channel 0 while the others leave the polarizer through output channel 1. The photons leaving through channel 1 are discarded and all the other photons are sent to Bob. The orientation ϕ_B of Bob’s polarizer switches randomly between $0^\circ(\rightarrow)$ and $45^\circ(\nearrow)$. These two directions define Bob’s two measurement basis, the rectilinear or diagonal linear basis.

As indicated in Table. 7.1, the probabilities to observe a photon in output channel 0 and 1 are $\cos^2(\phi_A - \phi_B)$ and $\sin^2(\phi_A - \phi_B)$, respectively. It is clear from Table 7.1 that the cases for which Bob has a definite outcome correspond to situation in

which Bob selected an observation basis that is consistent with the choice made by Alice.

In Table. 7.3, we show the first 100 bits of the sifted sequence, extracted from a simulation sequence of 10^5 events. After passing through Alice's polarizer, the number of the photons sent to Bob is 49920 (approximately 1/2 of the total number of events), and the length of the sifted key is 25072 (approximately 1/4 of the total number of events). From Table. 7.3, we see that the first 100 bits of the sifted key that Alice and Bob obtain are identical, as expected. We have checked that the other bits in the sifted key are identical also (results not shown). Furthermore, the simulation results for the sifted key do not depend the choice of the simulation model (PP or DP) for the polarizer (results not shown). The fidelity F , defined as the ratio of the correct bits in the sifted key to the length of the sifted key is 100%.

7.5.2 Simulation of the BB84 protocol in the presence of an eavesdropper

The presence of Eve is built into the simulation algorithm by adding a polarizer and implementing the intercept-resend strategy. Thereby, we assume that Eve intercepts all the photons that Alice sends to Bob and that she is able to perform the measurements in the same rectilinear or diagonal linear basis as the ones used by Bob. It is easy to see that for this type of eavesdropping, the error rate in the sifted key should be about 25%. In Table. 7.4, we show the first 100 bits of the sifted sequence, extracted from a simulation sequence of 10^5 events. The number of the photons that Bob receives is 50074 (approximately 1/2 of the total number of events), and the length of the sifted key is 25043 (approximately 1/4 of the total number of events). In this case, the fidelity is about 75.2%. As in the case without eavesdropper, the simulation results for the sifted key do not depend on the choice of the simulation model (PP or DP) for the polarizer (results not shown).

7.5.3 Misalignment of the measurement basis

In this section, we consider a situation in which there is a misalignment of the measurement basis of both parties.

In real experiments, it is unlikely that, say the rectilinear basis used by Alice is perfectly aligned with the rectilinear basis used by Bob. Furthermore, in real experiments the polarization of the photons changes as they propagate through the medium because of interactions with the medium (air, fibers). Moreover, for some strategies, the results of eavesdropping can be viewed as a rotation of Bob's measurement basis, making it more difficult to distinguish between a real misalignment

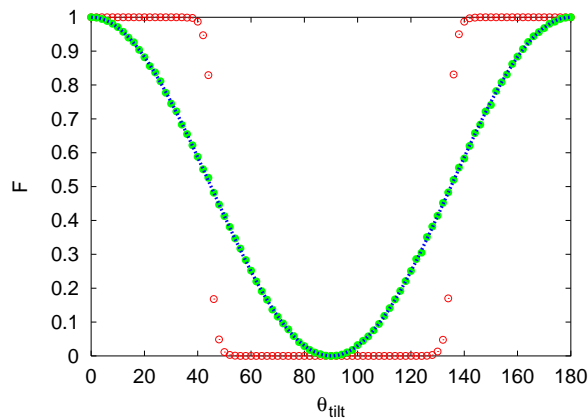


Figure 7.1: The fidelity F of the sifted key as a function of misalignment θ_{tilt} . Solid circles (green): Simulation data using the PP model. Open circles (red): Simulation data using the DP model. Dashed line (blue): Theoretical prediction given by Eq. (7.9).

of the basis and the presence of an eavesdropper. Thus, it is important to study the effects of misalignments of the coordinate systems.

In our simulations, we use the orientations of Alice’s polarizer as reference and tilt Bob’s basis by an angle θ_{tilt} . Therefore Bob’s basis changes to from 0° to $0^\circ + \theta_{\text{tilt}}$ and from 45° to $45^\circ + \theta_{\text{tilt}}$. In Fig. 7.1, we show our simulation results for the fidelity as a function of θ_{tilt} .

Unlike in the two previous cases, the simulation results for the sifted key depend on the choice of the simulation model (PP or DP) for the polarizer. For the PP model, the simulation data (solid circles in Fig. 7.1) is in good agreement with experimental results [146, 147]. For this model, we may compute the averaged fidelity by averaging (according to Malus’ law) the probabilities for obtaining identical bits in the sifted keys. We find

$$F_{PP} = \cos^2 \theta_{\text{tilt}}. \quad (7.9)$$

This function is shown as the dashed line in Fig. 7.1, demonstrating that there is excellent agreement between theory and simulation. The open circles in Fig. 7.1 are the simulation data as obtained with the DP model. Clearly, the sifted keys obtained by using the DP model are much more robust with respect to misalignments of the polarizers than the ones obtained by using the PP model. On the other hand, the DP results do not agree with currently available experimental results [146, 147], suggesting that the polarizers that are used in these experiments are not described by the DP model.

7.5.4 Discussion

Clearly, our simulation algorithm for the BB84 does not solve an equation of quantum theory nor does it rely on concepts of quantum theory. This should not come as a surprise: As quantum theory does not describe individual events (the quantum

measurement paradox) [1, 2], there is no reason to expect that quantum theory has any bearing on quantum cryptography, other than that it describes the averages over many events. As this point of view is in conflict with popular statements that quantum cryptography requires a full quantum mechanical description [135] or that quantum cryptography relies on the Heisenberg uncertainty relation, it is of interest to consider the question at which point concepts of quantum physics enter into our event-by-event simulation of the BB84 protocol.

From the description of the simulation algorithm, it is clear that in order for the BB84 to be secure, it is essential that the message and messenger have the following properties:

1. A message can be one out of two pairs of possible items only.
2. The messenger tells the recipient which of the two pairs the item that the messenger carries belongs to, but the messenger cannot tell a recipient which item it is.
3. The messenger can deliver the message only once and after delivering the message, the messenger self-destructs.

It is not too difficult to build a macroscopic device with these properties (minor modifications to intelligent containers used for transport of valuables and cash would do). Imagine that Alice has a set of boxes (the messengers) with the following properties:

1. Once closed, the box explodes when it is being tampered with. The box is shielded such that when it detects penetrating radiation, it explodes, making it impossible to analyze its content without destroying the content. Note that for secure quantum cryptography, similar conditions apply to Alice's and Bob's station too [135].
2. As long as the box is open, Alice can wire the electronics inside the box such that the electronic circuit encodes one of the four possibilities according to Table. 7.1. After wiring her bit, she closes the box and sends it to Bob.
3. On the outside, the box has a button and a switch, the setting of which corresponds to Bob's choice of the orientation of his measurements basis (see Table. 7.1). Bob puts the switch in one of its two positions and then he presses the button. The electronics inside the box, causes the box to explode immediately, after five seconds or after ten seconds, corresponding to the case where Bob detects a 0, ?, or 1, respectively (see Table. 7.1).

It is not difficult to see that this classical, macroscopic device is no less vulnerable to eavesdroppers than the quantum cryptography system. Of course, the latter is much more user-friendly and less expensive to operate.

7.6 Event-based simulation of the Ekert protocol

Starting from the observation that coincidence in time is a key ingredient in experimental realizations of the EPR *gedanken* experiment, several computer simulation algorithms have been proposed that (1) satisfy Einstein's conditions of local causality and realism and (2) exactly reproduce the two-particle correlation that is characteristic for a quantum system in the singlet state [21, 63, 69, 70]. These algorithms generate the data event-by-event, use integer arithmetic and elementary mathematics to analyze the data, and do not rely on concepts of probability theory or quantum theory.

In this Section, we use these algorithms to perform an even-by-event simulation of Ekert's quantum cryptography protocol. For the sake of brevity, we do not review all the details of the algorithms. The reader who is interested in these aspects should consult the original papers [21, 63, 69, 70] and Chapter 6.

7.6.1 Simulation of the Ekert protocol in the absence of an eavesdropper

A schematic diagram of the simulation procedure is shown in Fig. 7.2. In the simulation algorithm, the source generates pairs of particles (photons in the real experiment). Particle A and B travel to Alice and Bob, respectively. Each particle carries a two-dimensional unit vector given by

$$\begin{aligned} S_{n,1} &= (\cos \psi_n, \sin \psi_n), \\ S_{n,2} &= (-\sin \psi_n, \cos \psi_n). \end{aligned} \tag{7.10}$$

where n labels the number of the event. The vectors $S_{n,1}$ and $S_{n,2}$ represent the polarizations ψ_n and $\psi_n + \frac{\pi}{2}$ of the two photons that fly to Alice and Bob, respectively. The distribution of ψ_n is taken to be uniform over the interval $[0, 2\pi]$. Note that after projecting the vectors $S_{n,1}$ and $S_{n,2}$ onto dichotomic variables, the latter satisfy the conditions for deriving the Wigner inequality (see Appendix A).

When the particle arrives at Alice's (Bob's) station, labeled by $i = 1$ ($i = 2$), a random number is used to select the polarizer that will be used to perform the polarization measurement on the photon. This measurement maps the angle ψ_n onto the variable $x_{n,i} = x_{n,i}(\psi_n, A_{n,i}) = \pm 1$. Thus, the results of generating N of these events can be summarized by

$$\Gamma_{n,i} = \{x_{n,i} = \pm 1, A_{n,i} = \pm 1 | n = 1, \dots, N\}, \tag{7.11}$$

where $A_{n,i}$ denotes which of the polarizers has been selected. It is clear that we have assumed that the value of $x_{n,i}$ depends on the incoming polarization and the internal orientation of the selected polarizer only.

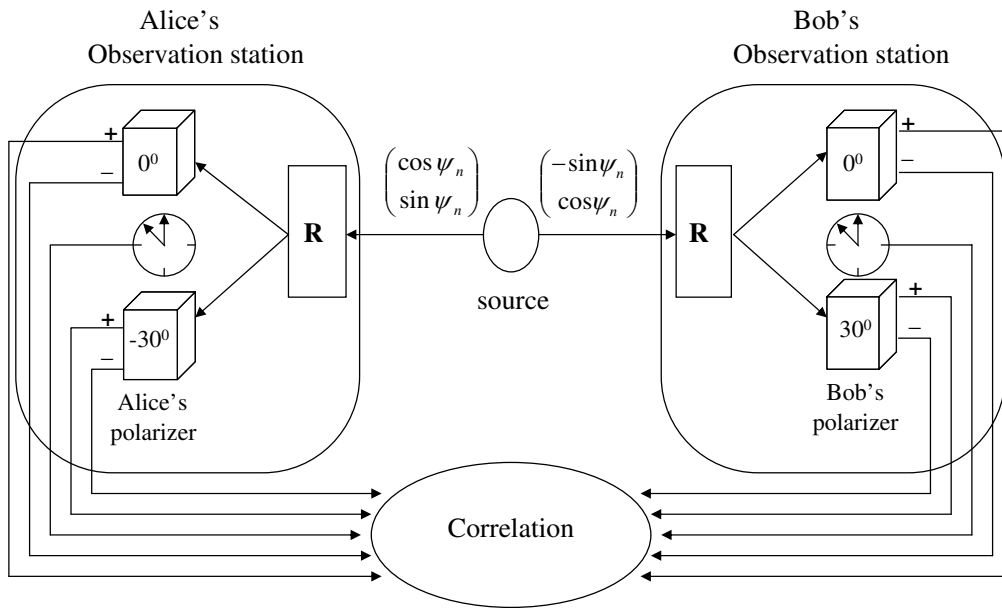


Figure 7.2: Schematic diagram of the event-by-event simulation of Ekert's quantum cryptography protocol, using the (modified) Wigner inequality as a guard against eavesdroppers. The source emits pairs of particles with orthogonal but random polarization. The particles fly to Alice's and Bob's observation station, respectively. The rectangular boxes labeled by R direct the particles to one of the two polarizers, using a binary pseudo-random number. When the particle emerges from a polarizer it generates a +1 or -1 event, and a clock is used to attach a time tag to this event. After collecting all events, Alice and Bob use time coincidence to correlate their data and to extract the key.

In any real experiment, one needs a criterion to decide whether two objects form a single two-particle system or whether they may be considered as two single-particle systems. EPR experiments are no exception to this [44, 45]. EPR experiments with photons use coincidence in time to identify a single pair of two photons. Note that time coincidences play an essential role in real quantum cryptography experiments [135].

In practice, Alice and Bob add time tags to their detection events in order to be able to count coincidences. As the optical components (polarizers) induce time delays, it is reasonable for a particle to experience a time delay when it passes through the detection system. To mimic this, we introduce the time delay into our simulation algorithm [21, 63, 69, 70]. At each station, we generate a time tag that depends on the local settings only. Then, we compare the difference between the two time tags with a certain time window W . If this difference is smaller than W , the detection events are considered to be coincident. Otherwise, they are discarded.

We assume that the maximum time delay $T_{n,i}$ for a particle passing through a polarizer depends only on the angle difference between the polarization of the incident particle and the internal orientation of the polarizer. For instance, on Alice's side,

we set $T_{n,1} = T_{n,1}(\psi_n - \phi_{A,i})$. The time tag $t_{n,i}$ itself is taken to be a pseudo-random number from the interval $[0, T_{n,1}]$ [21, 63, 69, 70]. Summarizing, the simulation algorithm generates two data sets

$$\Upsilon_{n,i} = \{x_{n,i} = \pm 1, A_{n,i} = \pm 1, t_{n,i} | n = 1, \dots, N\}, \quad (7.12)$$

for $i = 1$ (Alice) and $i = 2$ (Bob). The structure of these data sets is identical to the data sets collected in EPR experiments with photons [44, 45].

From Ref. [21, 63, 69, 70], we know that the simulation model can reproduce all the results of quantum theory of a system of two $S = 1/2$ particles if we take $T_{n,1}(\theta) = |\sin 2\theta|^d$ (note that we have chosen the maximum time delay as the unit of time). Here d is a free parameter, which we call the time-delay parameter. If $d = 0$, we have $T_{n,i} = 1$, implying that the maximum time delay does not depend on the relative orientation. In this case, the time delay has no essential influence on the final results [21, 63, 69, 70]. In our simulation (and also in experiment [44]), we first fix the time-tag resolution, denoted by $0 < \tau < 1$. Then, in our simulations, the time window is defined by $W = k\tau$, where k is an integer. It is clear that τ effectively determines the resolution by which we can resolve differences in the angles. After generating N pairs and collecting the data Eq. (7.12), we count the coincidences and we obtain an estimate for the probability

$$P_{++}(\phi_A, \phi_B) = \frac{C_{++}}{C_{++} + C_{--} + C_{+-} + C_{-+}}, \quad (7.13)$$

where $C_{xy} \equiv C_{xy}(\phi_A, \phi_B)$ denotes the number of coincidences between the signal $x = \pm 1$ at station 1 and a signal $y = \pm 1$ at station 2 for a fixed combination of ϕ_A and ϕ_B and is given by

$$C_{xy} = \sum_{n=1}^N \delta_{x,x_{n,1}} \delta_{y,x_{n,2}} \Theta(W - |t_{n,1} - t_{n,2}|). \quad (7.14)$$

From Eq. (7.13) we compute the Wigner parameter S according to Eq. (7.3).

We first show simulation results obtained by using the DP model. In Fig. 7.3 (left), we plot the probability $P_{++}(\phi_A, \phi_B)$ for fixed $\phi_A = 0$ and $0 \leq \phi_B \leq 2\pi$. The values of the other parameters used in the simulation are $k = 1$, $d = 2$, $\tau = 0.00025$, and $N = 10^8$. The dashed line in Fig. 7.3 (left) is the quantum theoretical prediction Eq. (7.4). From Fig. 7.3 (left), we conclude that there is an excellent agreement between the simulation data and quantum theory.

For comparison, in Fig. 7.3 (right) we present the simulation results for $d = 0$ and $d = 4$. For $d = 0$, the two time tags that we generated are just two independent uniform pseudo-random numbers between 0 and 1 and contain no information about the polarizations of the incident photons or the orientations of the polarizers. Therefore, because of the procedure to count coincidences, the size of the window can only influence the numbers of events we collect: W affects the statistical fluctuations

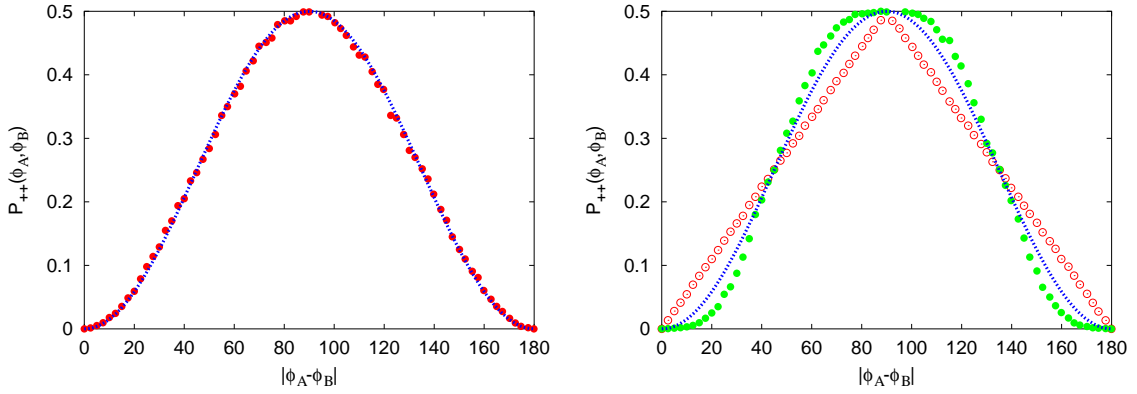


Figure 7.3: Left: $P_{++}(\phi_A, \phi_B)$ as a function of $|\phi_A - \phi_B|$. Solid circles: Simulation data obtained by using the DP model with $d = 2$. Dashed line: Quantum theory (Eq. (7.4)). Right: $P_{++}(\phi_A, \phi_B)$ as a function of $|\phi_A - \phi_B|$. Open circles: Simulation data by using the DP model with $d = 0$. Solid circles: Simulation data obtained by using the DP model with $d = 4$. Dashed line: Quantum theory (Eq. (7.4)).

only. As a check, we have taken a fairly large time window ($W = 100\tau$) and found that in this case, the distribution $P_{++}(\phi_A, \phi_B)$ is very close to the distribution that we find if we accept all the events (no coincidence window). For $d = 4$, we see from Fig. 7.3 (right) that the correlations are “stronger” than those of the quantum system [21, 63, 69, 70].

Next, we consider the Wigner parameter S for the fixed relation of the four orientations mentioned above: $\phi_{A,1} = \phi_{B,1} = \varphi$, $\phi_{A,2} = \varphi - \theta$, $\phi_{B,2} = \varphi + \theta$. Inserting these special values into Eq. (7.3) we get

$$S(\theta) = \sin^2 \theta - \frac{1}{2} \sin^2 2\theta. \quad (7.15)$$

Since in this case, the Wigner parameter depends on θ only, it is sufficient to consider the case $\varphi = 0$.

The simulation results are plotted in Fig. 7.4. The values of the parameters used in the simulation are $k = 1$, $d = 2$, $\tau = 0.00025$, and $N = 10^8$. Again, we see an excellent agreement between the simulation data and quantum theory. Furthermore, from Fig. 7.4 it is clear that the maximum violation of Wigner inequality is reached at $\theta = 30^\circ$. Therefore, in the Ekert protocol, the orientations of both parties are chosen to be $\phi_{A,1} = \phi_{B,1} = 0^\circ$, $\phi_{A,2} = 30^\circ$, $\phi_{B,2} = -30^\circ$. Then, the violation of the Wigner inequality signals the strong anti-correlation of the pairs and the Wigner parameter S can be used to quantify the security of the protocol.

For completeness, we show in Fig. 7.5 (left) the results for the Wigner parameter for the cases $d = 0$ and $d = 4$. As discussed above, $d = 0$ corresponds to the case for which correlations are computed without taking the time-tag information into account, showing “classical” correlations. For $d = 4$, the correlation is stronger than

Table 7.5: The first 100 bits of the sifted key of Ekert’s protocol without eavesdropping, as obtained by using the DP model. The upper part gives bits 0 – 50, the lower part gives bits 51 – 100. In this case, there are no errors in this part of the sifted key (the error rate is very low (10^{-5})).

Alice’s bits	1	1	1	0	0	0	1	0	0	1	1	0	1	1	1	1	1	1	0
Bob’s bits	1	1	1	0	0	0	1	0	0	1	1	0	1	1	1	1	1	1	0
Alice’s bits	1	0	0	0	0	0	1	0	0	0	0	1	0	1	1	1	0	1	0
Bob’s bits	1	0	0	0	0	0	1	0	0	0	0	1	0	1	1	1	0	1	0
Alice’s bits	1	1	1	1	0	1	0	1	0	1	1	0	0	1	0	1	1	0	0
Bob’s bits	1	1	1	1	0	1	0	1	0	1	1	0	0	1	0	1	1	0	0
Alice’s bits	0	1	0	0	1	0	0	0	1	1	0	1	0	0	1	0	1	1	0
Bob’s bits	0	1	0	0	1	0	0	0	1	1	0	1	0	0	1	0	1	1	0
Alice’s bits	0	1	1	0	0	1	1	0	1	0	0	0	0	0	0	1	0	0	0
Bob’s bits	0	1	1	0	0	1	1	0	1	0	0	0	0	0	0	1	0	0	0

Table 7.6: The first 100 bits of the sifted key of the Ekert protocol without eavesdropping, as obtained by using the PP model. The upper part gives bits 0 – 50, the lower part gives bits 51 – 100. The differences between Alice’s and Bob’s sifted key are emphasized by underlining the bits. There are only 2 errors in this part of the sequence.

Alice’s bits	0	0	0	0	0	0	1	1	0	1	0	0	1	0	1	0	1	0	1
Bob’s bits	0	0	0	0	0	0	1	1	0	1	0	0	1	0	1	0	1	0	1
Alice’s bits	1	1	0	0	1	0	<u>0</u>	1	0	0	0	1	0	0	1	0	0	1	1
Bob’s bits	1	1	0	0	1	0	<u>1</u>	1	0	0	0	1	0	0	1	0	0	1	1
Alice’s bits	0	1	1	1	1	0	0	0	1	1	1	1	1	0	0	0	1	0	1
Bob’s bits	0	1	1	1	1	0	0	0	1	1	1	1	1	0	0	0	1	0	1
Alice’s bits	0	0	0	1	0	1	1	<u>1</u>	0	0	1	1	0	0	0	0	0	0	1
Bob’s bits	0	0	0	1	0	1	1	<u>0</u>	0	0	1	1	0	0	0	0	0	0	1
Alice’s bits	0	0	1	0	0	1	0	1	1	0	1	0	0	0	1	0	0	0	1
Bob’s bits	0	0	1	0	0	1	0	1	1	0	1	0	0	0	1	0	0	0	1

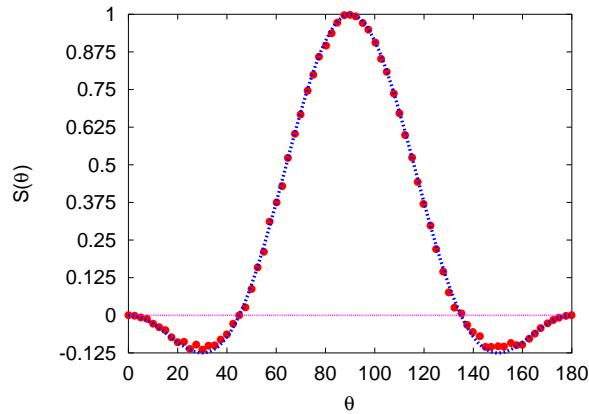


Figure 7.4: The Wigner parameter S as a function of θ . Solid circles: Simulation data obtained by using the DP model with $d = 2$. Dashed line: Quantum theory (Eq. (7.3)).

the one of the quantum system, hence the violation of the Wigner inequality can be larger.

Having established that our simulation algorithm reproduces the results of quantum theory of a single system of two polarizations, we now use the algorithm to simulate Ekert's quantum cryptography protocol.

As discussed earlier, the anticorrelated bits are generated using a parallel basis (that is, the basis selected by both parties is $\phi_{A,1} = \phi_{B,1} = 0^0$). After inverting all the bits from one of the two parties, we expect to obtain two identical sequences. The first 100 bits from a long simulation are shown in Table. 7.5. In this simulation, which uses the DP model, we observe an almost perfect anticorrelation of the two photons. Indeed, if $\phi_{A,1} = \phi_{B,1} = 0^0$, the relative error in the key is of the order of 10^{-5} .

Finally, we simulate this protocol by using the PP model. It is known that in order to reproduce the correct quantum correlations, we must take $d = 4$ [21, 70]. Except for the value of d , we take the same simulation parameters as in the DP-model simulations and repeat the calculation. The simulation results are shown in Fig. 7.5 (right).

After inverting all the bits from one of the two parties, we obtain two sequences of bit strings, the first 100 bits being shown in Table. 7.6. The error rate in this simulation is of the order of 10^{-2} . That this error rate is larger than in the DP simulation is easy to understand: If we use the PP model, the outcome of each individual measurement is inherently (pseudo-) random instead of deterministic as in the case of the DP model.

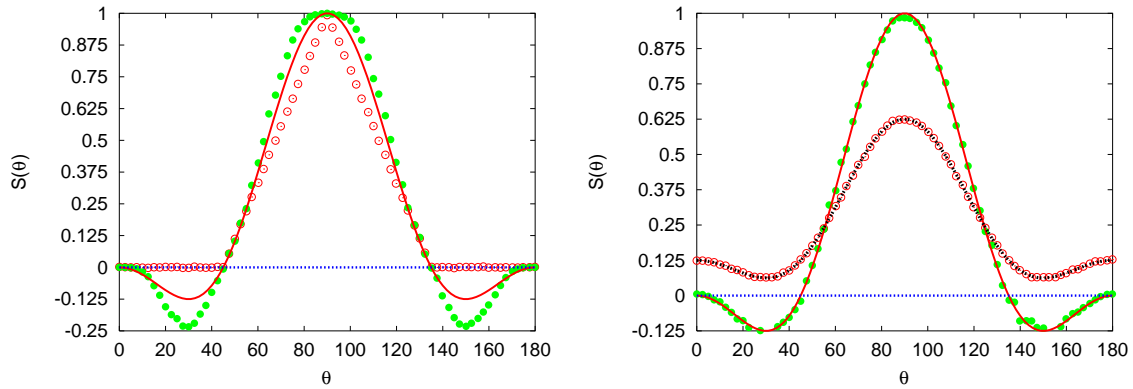


Figure 7.5: Left: The Wigner parameter S as a function of θ . Open circles: Simulation data obtained by using the DP model with $d = 0$. Solid circles: Simulation data obtained by using the DP model with $d = 4$. Solid line: Quantum theory (Eq. (7.3)). Right: The Wigner parameter S as a function of θ . Solid circles: Simulation data obtained by using the PP model with $d = 4$. Open circles: Simulation data obtained by using the PP model with $d = 0$. Dashed line: Quantum theoretical result for S (see Table. 7.2); Dashed line (black): Analytical results for S and $d = 0$.

7.6.2 Simulation of the Ekert protocol in the presence of an eavesdropper

In the previous subsection, we have demonstrated that by using the perfectly anticorrelated source, together with the time-tag model and a time window to count coincidences, we can reproduce the correlation that is characteristic for a quantum system in the singlet state. In this subsection, we simulate the situation in which an eavesdropper is present.

First, we consider the special case in which Eve uses two polarizers with fixed, perpendicular orientations: $\psi_A = 45^\circ$ and $\psi_B = 135^\circ$. We should imagine that Eve can put these polarizers on both sides of the source. Hence, she can manipulate the polarization that Alice and Bob will observe in their measurements.

Our simulation model can easily deal with this complication: We just put two PPs (or DPs) between the source and Alice and the source and Bob, respectively. We repeat the simulations as in the case without an eavesdropper and plot the two Wigner parameters S and S' as a function of θ .

In Fig. 7.6, we see two groups of curves with the same shape: The simulation result of S' (solid diamonds) and the quantum theoretical result of the modified Wigner parameter (solid line) agree very well. The simulation result of S (solid triangles) and the quantum theoretical result of the Wigner parameter (dashed line) are in excellent agreement too. Both the data for S and S' are larger than zero, signaling the presence of an eavesdropper. As $S' \geq S$, the modified Wigner parameter clearly is more powerful to disclose the eavesdropper.

Also shown in Fig. 7.6 is the fidelity of the sifted key as a function of θ . The

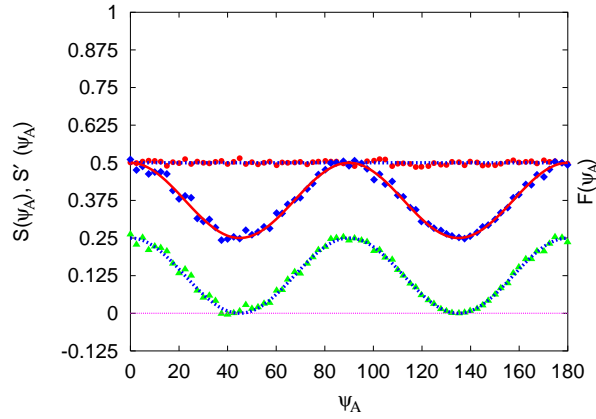


Figure 7.6: The fidelity F of the sifted key and the two Wigner parameters S and S' as a function of θ . Solid circles: Simulation data for F ; Dashed line: Quantum theoretical result for F ($F = 1/2$); Solid diamonds: Simulation data for S' ; Solid line: Quantum theoretical result for S' (see Table. 7.2); Solid triangles: Simulation data for S ; Dotted line (black): Quantum theoretical result for S (see Table. 7.2).

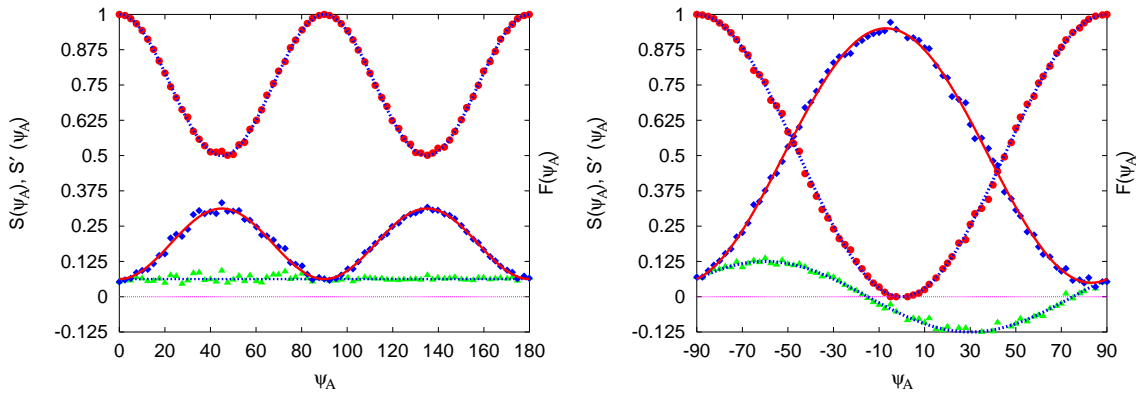


Figure 7.7: Left: The fidelity F and the two Wigner parameter S and S' as a function of ψ_A for the case $\psi_B = \psi_A + 90^\circ$. For the legend, see Fig. 7.6. Right: The fidelity F and the two Wigner parameter S and S' as a function of ψ_A for the case $\psi_B = 90^\circ$. For the legend, see Fig. 7.6.

simulation data for $F(\theta)$ lies on top of the theoretical expectation $F(\theta) = 1/2$. It is clear that the fidelity does not depend on the angle θ . In this case, the value of the fidelity is about 0.5 due to the choice of the orientations of Eve's polarizers.

Next, we take $\theta = 30^\circ$ (the optimal values for Ekert's protocol without eavesdropper) to study the dependence of the fidelity on the settings of Eve's polarizers. We consider two different situations: The first one is that Eve's polarizers always have perpendicular orientations. The second one is that we fix one of Eve's polarizers at $\psi_B = 90^\circ$, and change the other setting ψ_A gradually from 0° to 180° .

The results for the first case are shown in Fig. 7.7 (left). The upper curves show the dependence of the fidelity on the orientation of Eve's polarizer: The solid circles represent the simulation data and the dashed line is the theoretical result according

to Malus' law ($F = 1 - \frac{1}{2} \sin^2 2\psi_A$). The data in the middle are the simulation results (solid diamonds) and the quantum prediction (line) of the Wigner parameter S' . The bottom curves in Fig. 7.7 (left) show the simulation data and the theoretical result for the Wigner parameter S . Recall that in order to detect the presence of an eavesdropper, we must have $S > 0$ or $S' > 0$ for all ψ_A . Clearly, there is excellent agreement between theory and simulation.

The results for the second case are depicted in Fig. 7.7 (right). The legend is the same as in Fig. 7.6. Again, there is excellent agreement between theory and simulation. From Fig. 7.7 (right), it is clear that as $S < 0$ for some range of angles, using the Wigner parameter S would not allow Alice and Bob to recognize the existence of the eavesdropper, whereas if they use S' they can.

7.7 Summary

We present a new approach to simulate quantum cryptography protocols using event-based processes. The main feature of this approach is that it simulates the transmission of the individual bits by an event-based process. The algorithm that generates the events does not solve any quantum mechanical equation, thereby circumventing the fundamental problems arising from the quantum measurement paradox. Our simulation data for the BB84 and the Ekert protocol are, in all respects, in excellent agreement with the theoretical expectations. Extending the simulation method to account for effects such as depolarization by the medium (fibers, air) and noise is left for future research.

7.8 Appendix

Appendix A: Wigner inequality

We consider a two-particle system (particle A and B) and a pair of instruments that can measure a two-valued variable on each particle. The two possible values of the observed variable are taken to be ± 1 . Each instrument has a range of settings. For applications to quantum cryptography, it is sufficient to consider the special case for which particle A is detected using one of the two settings $\phi_{A,1}$ and $\phi_{A,2}$, and particle B is detected using the two settings $\phi_{B,1} = \phi_{A,1}$ and $\phi_{B,2}$. Each setting corresponds to a particular orientation of the apparatus that measures the polarization. It is assumed that the two observed results for a pair of particles are always opposite if the two instruments have the same setting. The Wigner inequality

$$P_{++}(\phi_{A,1}, \phi_{B,2}) + P_{++}(\phi_{A,2}, \phi_{B,1}) - P_{++}(\phi_{A,2}, \phi_{B,2}) \geq 0. \quad (7.16)$$

is a convenient tool to characterize the correlation between the results of the measurements on particles A and B .

Proof: For any combination of settings, for example, $\phi_{A,1}$ and $\phi_{B,2}$, the frequency of obtaining +1 on both sides is given by

$$F_{++}(\phi_{A,1}, \phi_{B,2}) = \frac{N_{++}(\phi_{A,1}, \phi_{B,2})}{N}, \quad (7.17)$$

where $N_{++}(\phi_{A,1}, \phi_{B,2})$ denotes the number of events for which both instruments yield +1 and N is the total number of events. For a different combination of the settings, the value of N is assumed to be the same (= ideal experiment assumption). We now show that

$$N_{++}(\phi_{A,1}, \phi_{B,2}) + N_{++}(\phi_{A,2}, \phi_{B,1}) - N_{++}(\phi_{A,2}, \phi_{B,2}) \geq 0, \quad (7.18)$$

holds under the conditions mentioned earlier.

Let us denote by $\phi_{A,1}^{(n)}$ and $\phi_{B,2}^{(n)}$ the results recorded for the i th pair using the settings $\phi_{A,1}$ and $\phi_{B,2}$. Then $N_{++}(\phi_{A,1}, \phi_{B,2})$ can be written as

$$N_{++}(\phi_{A,1}, \phi_{B,2}) = \sum_{n=1}^N \frac{1 + \phi_{A,1}^{(n)}}{2} \frac{1 + \phi_{B,2}^{(n)}}{2}. \quad (7.19)$$

If the settings of the two instruments are such that $\phi_{A,1} = \phi_{B,1}$ then we have $\phi_{A,1}^{(n)} = -\phi_{B,1}^{(n)}$ and

$$N_{++}(\phi_{A,1}, \phi_{B,1}) = \sum_{n=1}^N \frac{1 + \phi_{A,1}^{(n)}}{2} \frac{1 + \phi_{B,1}^{(n)}}{2} = 0. \quad (7.20)$$

Hence, instead of proving Eq. (7.18), we can equally well prove that

$$\begin{aligned} N_{++}(\phi_{A,1}, \phi_{B,2}) &+ N_{++}(\phi_{A,2}, \phi_{B,1}) - N_{++}(\phi_{A,2}, \phi_{B,2}) \\ &- N_{++}(\phi_{A,1}, \phi_{B,1}) \geq 0. \end{aligned} \quad (7.21)$$

Substituting Eq. (7.19) into Eq. (7.21) we obtain

$$\begin{aligned} \sum_{n=1}^N [(1 + \phi_{A,1}^{(n)})(1 + \phi_{B,2}^{(n)}) + (1 + \phi_{A,2}^{(n)})(1 + \phi_{B,1}^{(n)}) \\ - (1 + \phi_{A,2}^{(n)})(1 + \phi_{B,2}^{(n)}) - (1 + \phi_{A,1}^{(n)})(1 + \phi_{B,1}^{(n)})] \geq 0. \end{aligned} \quad (7.22)$$

After simplification, we find

$$\sum_{n=1}^N (\phi_{A,2}^{(n)} - \phi_{A,1}^{(n)})(\phi_{B,2}^{(n)} - \phi_{B,1}^{(n)}) \geq 0. \quad (7.23)$$

Making use of the assumption that $\phi_{A,1}^{(n)} = -\phi_{B,1}^{(n)}$, we find that $(\phi_{A,2}^{(n)} - \phi_{A,1}^{(n)})(\phi_{B,2}^{(n)} - \phi_{B,1}^{(n)}) \geq 0$. Hence, inequality Eq. (7.23) holds and so do inequalities Eqs. (7.21) and (7.18).

In the proof of Eq. (7.18), it has been assumed that the observations $\{\phi_{A,1}^{(n)}|n = 1, \dots, N\}$, $\{\phi_{A,2}^{(n)}|n = 1, \dots, N\}$, $\{\phi_{B,1}^{(n)}|n = 1, \dots, N\}$, and $\{\phi_{B,2}^{(n)}|n = 1, \dots, N\}$ do not depend on whether we record $N_{++}(\phi_{A,1}, \phi_{B,2})$, $N_{++}(\phi_{A,2}, \phi_{B,1})$, or $N_{++}(\phi_{A,2}, \phi_{B,2})$. In a computer simulation, it is a simple matter to satisfy this assumption because we have perfect control over the pseudo-random numbers that are used to generate the events but in real experiments, the validity of this assumption cannot be taken for granted.

Having shown that

$$F_{++}(\phi_{A,1}, \phi_{B,2}) + F_{++}(\phi_{A,2}, \phi_{B,1}) - F_{++}(\phi_{A,2}, \phi_{B,2}) \geq 0, \quad (7.24)$$

and assuming that the observations $\{\phi_{A,1}^{(n)}|n = 1, \dots, N\}$, $\{\phi_{A,2}^{(n)}|n = 1, \dots, N\}$, $\{\phi_{B,1}^{(n)}|n = 1, \dots, N\}$, and $\{\phi_{B,2}^{(n)}|n = 1, \dots, N\}$ are independent random variables, we may invoke the law of large numbers [77] to argue that for $N \rightarrow \infty$, $F_{++}(\phi_{A,1}, \phi_{B,2}) \rightarrow P_{++}(\phi_{A,1}, \phi_{B,2})$ with probability one. Under these assumptions, the Wigner inequality Eq. (7.16) holds.

Appendix B: Modified Wigner inequality

The proof of the modified Wigner inequality

$$P_{++}(\phi_{A,1}, \phi_{B,2}) + P_{++}(\phi_{A,2}, \phi_{B,1}) + P_{--}(\phi_{A,1}, \phi_{B,1}) - P_{++}(\phi_{A,2}, \phi_{B,2}) \geq 0, \quad (7.25)$$

is very similar to the proof of the original Wigner inequality. The essential difference is that the modified Wigner inequality holds if we drop the assumption of perfect anticorrelation.

Adopting the same strategy as in Appendix A, we have to prove that

$$N_{++}(\phi_{A,1}, \phi_{B,2}) + N_{++}(\phi_{A,2}, \phi_{B,1}) + N_{--}(\phi_{A,1}, \phi_{B,1}) - N_{++}(\phi_{A,2}, \phi_{B,2}) \geq 0. \quad (7.26)$$

Using Eq. (7.19), we can rewrite Eq. (7.26) as

$$\begin{aligned} & \sum_{n=1}^N [(1 + \phi_{A,1}^{(n)})(1 + \phi_{B,2}^{(n)}) + (1 + \phi_{A,2}^{(n)})(1 + \phi_{B,1}^{(n)}) \\ & \quad + (1 - \phi_{A,1}^{(n)})(1 - \phi_{B,1}^{(n)}) - (1 + \phi_{A,2}^{(n)})(1 + \phi_{B,2}^{(n)})] \geq 0. \end{aligned}$$

After simplification, we find

$$\sum_{n=1}^N [2 + \phi_{B,2}^{(n)}(\phi_{A,1}^{(n)} - \phi_{A,2}^{(n)}) + \phi_{B,1}^{(n)}(\phi_{A,1}^{(n)} + \phi_{A,2}^{(n)})] \geq 0. \quad (7.27)$$

It is easy to see that

$$2 + \phi_{B,2}^{(n)}(\phi_{A,1}^{(n)} - \phi_{A,2}^{(n)}) + \phi_{B,1}^{(n)}(\phi_{A,1}^{(n)} + \phi_{A,2}^{(n)}) \geq 0, \quad (7.28)$$

always holds. Hence, inequality Eq. (7.26) holds. Invoking the same arguments that were used to replace frequencies by probabilities in Appendix A, it then follows that inequality Eq. (7.25) holds.